

To be submitted to Concrete Science and Engineering (August, 1999)

# New effective medium theory for the diffusivity or conductivity of a multi-scale concrete microstructure model

E.J. Garboczi

National Institute of Standards and Technology  
Building Materials Division  
100 Bureau Drive, Stop 8621  
Gaithersburg, Maryland 20899-8621 USA

J.G. Berryman

Lawrence Livermore National Laboratory  
P. O. Box 808 L-200  
Livermore, CA 94551-9900

## Abstract

To attempt to represent concrete properly as a composite material, one must consider at least three phases: matrix, aggregates, and the interfacial transition zone (ITZ), a thin shell of altered matrix material surrounding each aggregate grain. Assigning each of these phases a different transport parameter, diffusivity or conductivity, results in a complicated composite transport problem. Random walk simulations can be performed for this system, but are time-consuming, hence the anticipated usefulness of effective medium theory. But, previous applications of differential effective medium theory were plagued by the need to use an arbitrary parameter chosen to fit the simulation results. A new kind of differential effective medium theory is presented in this paper that removes this need for a fitting parameter. An aggregate particle with a surrounding ITZ is mapped onto an effective particle of uniform conductivity, which is then treated in regular differential effective medium theory. The results of this theory are compared to random walk simulations for multi-scale concrete models with varying aggregate size distributions.

# 1 Introduction

Concrete is a composite material. It is made up of, at first sight, a cement paste matrix and aggregate grains of various sizes, ranging from the very smallest sand grains of diameter  $100\mu\text{m}$ , to the large aggregates of diameter  $10 - 20$  mm. However, upon closer examination, one finds a thin layer of matrix material surrounding each aggregate grain, called the interfacial transition zone (ITZ), where the cement paste matrix is different, usually more porous, than the bulk of the surrounding cement paste matrix. The ITZ has an average width of about the median cement particle size [1], and arises mainly from the “wall effect,” where cement particles are constrained by the aggregate surface to pack less efficiently in the ITZ. Typical widths of the ITZ are in the range  $10 - 30\mu\text{m}$ . Figure 1 gives a 2-D schematic view of a concrete with two sizes of particles to show the type of microstructure that must be considered.

So to attempt to represent concrete properly as a composite material, at least three phases must be considered, consisting of matrix, aggregates, and the ITZ regions. Assigning each of these phases a different transport parameter, diffusivity or conductivity, then results in a complicated composite transport problem. By conductivity is meant either thermal or electrical conductivity. In the diffusivity problem, which is the main problem of interest of these three to concrete [2], the aggregates have diffusivities of zero, while the ITZ and the matrix have in general different and non-zero diffusivities. The language of conductivity will be used throughout the remainder of this paper, but the diffusivity problem is exactly mathematically analogous, along with other physical problems [3, 4]. The equivalent elastic problem is of interest as well, but is outside the scope of this paper [5].

Of course, the real problem is more complicated still. The ITZ region in fact has a gradient of properties, since the porosity is a gradient from the aggregate surface outwards [6, 7, 8]. The dilute limit, with a single spherical aggregate surrounded by a spherically symmetric gradient of properties, can be handled exactly [9, 10, 11]. But the real microstructure of concrete, with a wide size distribution of aggregates each surrounded by overlapping gradients of properties, is too difficult to treat analytically, by numerical methods, or by effective medium theory. However, it has been shown that a multi-scale model can be used in order to map this very complicated microstructure into a simpler, but still complicated, microstructure, where the ITZ regions can be treated theoretically as a region of uniform properties [2, 9, 12]. This multi-scale, multi-step approach [2, 9, 12]. assigns the best value of ITZ thickness, which is the same for all aggregates, and conductivity, which is the same for all ITZ regions, to match the real material. Once this multi-scale procedure has been carried out, one ends up with a system as shown in Fig. 1, where the ITZ regions have uniform properties.

To compute the overall conductivity of the system shown in Fig. 1, random walk sim-

ulations have been performed [2, 13, 14]. Uncorrelated mathematical walkers (points) are thrown down at random, and then undergo random walks. Walkers that initially land in the aggregates do not move, and are not counted. A “clock” is maintained for each walker. The walkers move at different speeds depending on which phase they are in. The slope of the average root-mean-squared distance vs. time curve is then used to extract the overall conductivity or diffusivity. These are accurate and simple, but time-consuming, computations. The hope is to use some kind of effective medium theory (EMT) to replace the random walk simulations. This is done to reduce the computer time that is necessary to evaluate this step of the multi-scale model [12], so that the model becomes more widely used. However, the existence of accurate simulations is still required in order to validate the EMT results.

Previous applications of differential effective medium theory (D-EMT) [12] agreed fairly well with the random walker computations, but were plagued by having to use an arbitrary parameter that was fit to the result of simulations. The point of this paper is to derive a new kind of D-EMT that has no adjustable parameters. After introducing standard D-EMT, and deriving this new kind of D-EMT, the results of this new D-EMT are compared with the results of random walk computations on various concrete models [2, 12, 13], and are found to agree better with the simulations than did the old D-EMT.

## 2 Differential effective medium theory and effective particle mapping

Differential effective medium theory (D-EMT) [15] was chosen as the best candidate for the concrete problem as shown in Fig. 1 for the following reason. The accuracy of an EMT is often linked to how well its percolation properties match that of the experimental system being considered [14, 16]. In D-EMT, the inclusions are always discontinuous, and the matrix is always continuous. This is the same situation for concrete, with discontinuous aggregates embedded in a continuous matrix. So it might be expected that D-EMT would work well for concrete.

One should note, however, that several modeling studies have shown that in a typical concrete, the ITZ regions are themselves percolating [17, 18]. The form of D-EMT considered in this paper will not reflect this fact, although it will take the ITZ into account. However, whether or not percolation of a phase matters to the overall properties depends on the contrast of its properties with the surrounding phases [7, 19]. For the case of diffusion through concrete, the ITZ property is at most ten times that of the matrix, which is not enough of a contrast for percolation to matter particularly [7]. So this deficiency in D-EMT should not significantly affect the ability of D-EMT to be accurate for this problem. However, if the problem of fluid permeability were being considered [7], where the contrast between

ITZ and matrix is on the order of 100, then most likely D-EMT would fail, as the percolation of the ITZ regions would then matter greatly. Any approach not taking this into account is unlikely to be accurate.

## 2.1 Standard D-EMT

In the usual D-EMT, [15], when a particle with conductivity  $\sigma_p$  is embedded in a matrix with conductivity  $\sigma_{bulk}$ , the dilute limit is used to generate an approximate equation that can be solved for the effective conductivity. In the dilute limit, the value of  $c$ , the volume fraction of aggregates, is small enough so that the aggregate grains do not influence each other. The effective conductivity,  $\sigma$ , is then given exactly by [3, 14]:

$$\sigma = \sigma_{bulk} + \sigma_{bulk} m c + O(c^2) \quad (1)$$

where  $m$  is a dimensionless coefficient often called the dilute limit slope that is a function of the shape of the particle, and the ratio  $\frac{\sigma_p}{\sigma_{bulk}}$ . The higher order terms in the  $c$  expansion come from interactions between aggregate particles, and so are negligible in the dilute limit.

The dilute limit is now used to generate a differential equation for the conductivity when an arbitrary amount of aggregates is placed in the matrix. Suppose that a non-dilute volume fraction  $c$  of aggregates (of conductivity  $\sigma_p$ ) have been placed in the matrix. The effective conductivity of the entire composite system is now  $\sigma$ . This system of matrix (volume fraction =  $\phi$   $1 - c$ ) plus aggregates (volume fraction =  $c$ ) is thought of as being a homogeneous material. Suppose then that additional aggregates are added by removing a differential volume element,  $dV$ , from the homogeneous material, and replacing it by an equivalent volume of aggregates. The new conductivity,  $\sigma + d\sigma$ , is assumed to be given by the dilute limit

$$\sigma + d\sigma = \sigma + \sigma m(\sigma) \frac{dV}{V} \quad (2)$$

where  $V$  is the total volume and  $m(\sigma)$  is the same as that in eq. (1), but with  $\sigma_{bulk} \rightarrow \sigma$ . This is the key approximation that is made in order to generate the D-EMT. When the volume element  $dV$  was removed, only a fraction  $\phi$  was matrix material so that the actual change in the matrix volume fraction,  $d\phi$ , is given by

$$d\phi = -\phi \frac{dV}{V} \quad (3)$$

Eq. (2) then reduces to

$$d\phi/\phi = -d\sigma/(\sigma m(\sigma)), \quad (4)$$

which can be integrated to yield

$$-\int_{\sigma_{bulk}}^{\sigma} \frac{d\sigma'}{m(\sigma')\sigma'} = \int_1^{\phi} \frac{d\phi'}{\phi'} = \ln(\phi) . \quad (5)$$

For spherical aggregates of only one size, with conductivity  $\sigma_p$ , and embedded in a matrix of conductivity  $\sigma$ ,

$$m(\sigma) = 3 \frac{(\sigma_p - \sigma)}{(2\sigma + \sigma_p)} \quad (6)$$

The integral in eq. (5) can be done exactly, using eq. (7), with the result

$$\frac{(\sigma - \sigma_p)}{(\sigma_{bulk} - \sigma_p)} \left( \frac{\sigma}{\sigma_{bulk}} \right)^{-1/3} = (1 - c) \quad (7)$$

where  $\sigma'$  is the matrix phase conductivity at any point in the D-EMT calculation.

## 2.2 Including the ITZ in the dilute limit

In the concrete problem, as was mentioned in the Introduction, each aggregate is surrounded by a thin shell of different material, called the ITZ. Since any D-EMT is built up from the exact dilute limit, the dilute limit for such a composite particle is now discussed.

Consider an idealized aggregate particle, like those shown in Fig. 1. Real aggregates have non-spherical shape, but for many kinds of aggregates, a spherical shape is a reasonable approximation. A spherical shape is used in the multi-scale model [2, 12]. Consider spherical aggregate particles of conductivity  $\sigma_{agg}$  and radius  $b$ , each surrounded by a concentric shell of thickness  $h$  and conductivity  $\sigma_{ITZ}$ ,  $a = b + h$ , and all embedded in a matrix of conductivity  $\sigma_{bulk}$ . The left side of Fig. 2 shows these parameters pictorially. The volume fraction of aggregate grains, not counting the ITZ regions, which are only modified (more porous) matrix material, is still denoted by  $c$ . Eq. (1) is still valid, but now the slope  $m$  for the linear term in  $c$  is given exactly by [14, 21]

$$m = 3\alpha \frac{[(\sigma_{agg} - \sigma_{ITZ})(2\sigma_{ITZ} + \sigma_{bulk}) + \alpha(\sigma_{agg} + 2\sigma_{ITZ})(\sigma_{ITZ} - \sigma_{bulk})]}{[2(\sigma_{agg} - \sigma_{ITZ})(\sigma_{ITZ} - \sigma_{bulk}) + \alpha(\sigma_{agg} + 2\sigma_{ITZ})(\sigma_{ITZ} + 2\sigma_{bulk})]} \quad (8)$$

The parameter  $\alpha$  is defined by the radius of the particle and the thickness of the ITZ:

$$\alpha = \frac{(b + h)^3}{b^3} \quad (9)$$

When  $\sigma_{agg} = 0$ , the usual case for concrete, then eq. (8) becomes

$$m = \frac{3}{2}\alpha \frac{[2\sigma_{ITZ}(\alpha - 1) - \sigma_{bulk}(1 + 2\alpha)]}{[\sigma_{ITZ}(\alpha - 1) + \sigma_{bulk}(1 + 2\alpha)]} \quad (10)$$

This slope is negative when

$$\sigma_{ITZ} < \sigma_{ITZ} \frac{(1 + 2\alpha)}{2(\alpha - 1)} \quad (11)$$

and is positive otherwise. For most concrete cases, the slope  $m$  is negative when averaged over all particle sizes, as is discussed next. In all cases considered in this paper, the slope  $m$

was always negative, so there were no difficulties with having a zero value in the denominator of eq. (5).

Concrete has a size distribution of aggregate grain radii  $\{b_j\}$ , while the value of  $h$  is essentially fixed [2, 12]. That implies that the slope  $m_j$  for each kind of particle will be a function of  $b_j$ , because the parameter  $\alpha_j = [(b_j + h)/b_j]^3$  will be different for each particle. The aggregate size distribution is usually given by a sieve analysis characterized by  $d_i$ ,  $f_j$ ,  $i = 1, M + 1$ ,  $j = 1, M$ , where  $M$  is the number of sieves used,  $d_i < d_{i+1}$  is the endpoint diameters of the sieves, and  $f_j$  is the fraction of the total aggregate volume that is taken up in the  $j$ -th sieve ( $\sum_j f_j = 1$ ). For now assume that all the particles in the  $j$ -th interval have the same radius,  $b_j(d_j, d_{j+1})$ . Later on, this assumption will be relaxed.

The dilute limit is then defined the same way, but the slope used,  $\langle m \rangle = \sum_j f_j m_j$ , is first averaged over the aggregate particle size distribution (sieve analysis) before being used in the dilute limit formula. The slope  $m_j$  for the  $j$ -th size class is given by eq. (8), but with  $\alpha$  going to  $\alpha_j = \frac{(b_j+h)^3}{b_j^3}$ .

### 2.3 New D-EMT

The standard D-EMT is a two-phase theory. In the present case, the ITZ zone causes conceptual problems, since it introduces a third phase. To use D-EMT in this case, should the ITZ be treated as part of the particle, or should it be considered part of the matrix? If the ITZ conductivity is given independently of the matrix, then it should stay the same as the matrix is renormalized in the D-EMT calculation process. However, if it is given in terms of a ratio with the matrix conductivity, then if the ratio stays the same during the calculation process, then the absolute value of the ITZ conductivity will change [12]. The form of D-EMT previously used for the concrete problem [12] took a weighted average between these two cases, with the weights determined by a fit to random walk computations. The agreement with computations was not spectacular (20%), and there was no guarantee that the fitted weights would be the same for all concrete systems studied.

An answer to the conceptual dilemma stated above would be to construct a version of D-EMT in which the ITZ regions were either unambiguously aggregate or matrix. This would eliminate the need for adjustable parameters. Since the ITZ regions, disregarding overlaps, are the same shape as the spherical aggregate particles, one is drawn to the option of making the ITZ regions part of the aggregates. The way this can be done is according to the following idea: Map each aggregate particle plus its accompanying ITZ region into a single effective particle, with an effective uniform conductivity,  $\sigma_p$ , which is embedded in the bulk matrix. This idea is illustrated in Fig. 2. The radius of this effective particle will then be  $a_j = b_j + h$ , rather than simply  $b_j$ . This procedure can be carried out by equating the exact result for  $m_j$ , eq. (8), to the exact result for  $m_j$  when the particle is uniform.

The dilute limit slope  $m_j$  for a spherical particle of conductivity  $\sigma_p$ , radius  $b_j + h$ , embedded in a matrix of conductivity  $\sigma_{bulk}$ , is given by

$$m_j = 3\alpha_j \frac{(\sigma_p - \sigma_{bulk})}{(2\sigma_{bulk} + \sigma_p)} \quad (12)$$

**\*\*clarify\*\*** where  $c$  is still the volume fraction of aggregates only (see eq. (1)). If this dilute limit is equated to eq. (8), the value of  $\sigma_p$  turns out to be

$$\sigma_p = \frac{[2(\sigma_{agg} - \sigma_{ITZ}) + \alpha_j(\sigma_{agg} + 2\sigma_{ITZ})]\sigma_{ITZ}}{[-(\sigma_{agg} - \sigma_{ITZ}) + \alpha_j(\sigma_{agg} + 2\sigma_{ITZ})]} \quad (13)$$

Therefore, the dilute limit for a particle of radius  $b_j + h$ , with conductivity  $\sigma_p$  (which is a function of  $j$ ), referred to the volume fraction of aggregate  $c$ , is the same as for the real particle, of radius  $b_j$  and conductivity  $\sigma_{agg}$ , and accompanying ITZ of thickness  $h$  and conductivity  $\sigma_{ITZ}$ . Figure 3 shows this mapping between  $\sigma_p$  and the ITZ conductivity, for four different diameter (radius =  $2b$ ) aggregate particles, where  $\sigma_{agg} = 0$ , and  $h = 20\mu\text{m}$ . The dependence on the value of  $\alpha$  and thus the particle size can be clearly seen.

This effective particle is then treated in regular differential effective medium theory, as described above. When an aggregate size distribution is used, the function  $m(\sigma)$  is an average over this size distribution, as was stated above. The integral can be done numerically for chosen values of  $\sigma$ , with the aggregate volume fraction  $c = 1 - \phi$  then treated as being a function of  $\sigma$ . There are a few differences, however, involving the effective aggregate volume fraction. Each particle is now of radius  $b_j + h$ , so that the volume fraction of “effective aggregate” now goes to  $c'$ , not  $c$ . The value of  $c'$  must be known in order to perform the integral in eq. (5).

These differences can be worked out simply by considering the number of particles of a certain type. If  $V_i$  is the total volume of the  $i$ -th kind of particle, and  $N_i$  is the total number of this kind of particle, then

$$N_i \frac{4\pi}{3} (b_i)^3 = V_i \quad (14)$$

and therefore

$$\frac{N_i}{V} \frac{4\pi}{3} (b_i)^3 = \frac{V_i}{V} = f_i c \quad (15)$$

$$n_i \frac{4\pi}{3} (b_i)^3 = f_i c \quad (16)$$

where  $V$  is the total volume of the system and  $n_i$  is the number of particles of type  $i$  per unit volume.

Now the new values of  $f_i$  and  $c$ ,  $f'_i$  and  $c'$ , are defined via rewriting the previous equation:

$$n_i \frac{4\pi}{3} (b_i + h)^3 = f'_i c' \quad (17)$$

The values of  $f'_i$  and  $c'$  can also be defined directly by

$$c' = \sum_{j=1}^M n_j \frac{4\pi}{3} (b_j + h)^3 \quad (18)$$

$$f'_i = \frac{n_i (b_i + h)^3}{\sum_{j=1}^M n_j (b_j + h)^3} \quad (19)$$

By combining the above equations, one can then derive forms for  $f'_i$  and  $c'$  that involve only  $f_i$ ,  $c$ ,  $h$ , and  $\alpha_i$ :

$$f'_i = \frac{c_i \alpha_i}{\sum_{j=1}^M f_j \alpha_j} \quad (20)$$

$$c' = c \sum_{j=1}^M f_j \alpha_j \quad (21)$$

It should be noted that while the value of  $c$  was for non-overlapping aggregate particles, the value of  $c'$  is for the volume occupied by each aggregate particle and its surrounding ITZ region, where the ITZ regions are assumed to not overlap. In a real concrete, these ITZ regions do overlap, causing percolation phenomena, as was mentioned earlier. This treatment of the ITZ volume fraction is another approximation of the D-EMT method.

In summary, a D-EMT calculation is carried out as follows. First the sieve analysis is used to compute  $c'$  and  $f'_i$ . Then the integral in eq. (5) is carried out numerically by Gaussian quadratures [22], where  $\langle m \rangle$  is numerically averaged over the sieve analysis. Since the diameter range of each sieve is rather large, the assumption is made that within each sieve, the particles are uniformly distributed by volume, thus relaxing the assumption made earlier that all particles in a certain sieve had the same radius (see Sec. 2.2). This enables an integral to be performed over each bin, and then a summation over all the sieves ( see Appendix 2 in Ref. [12]). This procedure is also used to compute  $c'$  and  $f'_i$  as well. The actual FORTRAN software used to calculate the D-EMT for an arbitrary sieve analysis is available on the Internet [23].

### 3 Results

Random walk simulation data are available for the multi-scale concrete model for several aggregate size distributions (sieve analyses) and a number of choices of the conductivity contrast between ITZ and matrix [2, 12]. In these data, the aggregates always had zero



conductivity ( $\sigma_{agg} = 0$ ). The random walk simulation data is accurate to within a few percent, so it can be used to check the results of the new D-EMT. If the new D-EMT is able to replace these lengthy simulations by achieving an accuracy of 10 – 20%, that would be a successful application. Experimental measurements, which the multi-scale theory hopes to predict, are probably only accurate to within a factor of two [2].

Table 1 shows the values  $c_i$  of the four different sieve analyses used (cfcc, fffc, ffcc, and cffc, see Ref. [2] for details of these sieve analyses). Figure 4 shows the results of the new D-EMT, plotted against the data of Table 2, taken from Ref. [2]. Good agreement, 10% or better, is seen for most of the values, with somewhat higher disagreement but still less than 20% for some data points. It is interesting to note that most of the D-EMT results are systematically lower than the simulation results. This is probably at least partly an artifact of the D-EMT calculation, because even at fairly low contrast, the percolation of the ITZ regions will have some effect. It is also possible that the simulation results are a bit high, which would be the case if the random walkers were not allowed to run long enough. The random walkers start out diffusing at the matrix diffusivity, and only gradually, through colliding with many aggregates, does their effective diffusivity and conductivity come down to the concrete value. Spot checks of some of the random walk data indicate that the random walk values would become about 5% lower with more random steps being made, which would significantly improve the agreement with the new D-EMT [20].

A second set of simulation data has recently become available [13], for models with volume fractions of aggregate of 0.62 and 0.70, and a range of conductivity values for the ITZ region, with  $\sigma_{ITZ}/\sigma_{bulk}$  both less than and greater than unity. The sieve analysis for these systems is shown in Table 3. Table 4 shows the simulation and D-EMT data for the different concrete mixtures and parameter choices. Good agreement with simulation is shown for all parameter values, with the differences well below 10% for most of the data, and only a few differences as high as 13%.

Figure 5 shows the D-EMT data plotted against the simulation data from Table 4. The dashed line is the line of equality. The data points are seen to follow the dashed line quite well. The D-EMT predictions are mostly again seen to err on the small side, being slightly under the real values. It is interesting to note that even for values of  $\sigma_{ITZ}/\sigma_{bulk} \simeq 20$ , the D-EMT still agrees very well with the random walker data.

Figure 6 shows the same data as in Table 4, but now plotted as a function of  $\sigma_{ITZ}/\sigma_{bulk}$ , separately for the 0.62 and 0.70 aggregate volume fraction concrete systems. The D-EMT correctly captures the shape of these curves [13, 21].

## 4 Discussion and Summary

One should note that the aggregate sieve analyses given in Table 1 involve extremal values of recommended concrete mixtures [2, 24], while the sieve analysis given in Table 3 is from the middle of the range recommended for the aggregate size distributions [13, 24]. It is comforting to note that the D-EMT seems to work somewhat better for the usual concrete mixture designs, rather than for unusual values.

As was stated in the Introduction, concrete is actually even more complicated than the three-phase system discussed in this paper, for several reasons. First, aggregates are only approximately spherical. Second, the ITZ has a gradient of properties extending out to its width, and is not a uniform property shell [9]. And third, concrete is an *interactive* composite, where the amount of aggregates affects the properties of the matrix [12, 7]. For these reasons, a multi-scale approach has been taken to model concrete diffusivity/conductivity. In part of this model, the actual ITZ microstructure near an aggregate, as well as the global arrangement of ITZ regions, is used both to map the ITZ gradient into a uniform property region, and to derive an accurate value of the ratio of ITZ to bulk matrix properties. By doing this multi-scale procedure carefully, the best value of the ITZ thickness and conductivity are used. It is known that the ITZ thickness and conductivity, when mapping onto a uniform property shell, are not independent of each other [9].

In the multi-scale model, the conductivity of the resulting three-phase effective microstructure was computed using random walk simulations. The reason for developing an improved D-EMT was to replace these rather lengthy random walk simulations [12, 2]. The random walk part is CPU time-intensive, and a fairly simple formula, or algorithm, that could give 10-20% accuracy for the usual range of concrete mixtures studied would be very useful. The new D-EMT derived in this paper seems to fit the requirements, and should be able to serve as a routine replacement for the random walk simulations in the multi-scale microstructural model for predicting concrete diffusivity.

## Acknowledgments

We thank the Partnership for High Performance Concrete Technology of the Building and Fire Research Laboratory for partial support of the work of EJG, and the National Science Foundation Science and Technology Center for Advanced Cement-Based Materials for supporting an annual computer modeling workshop (see <http://ciks.cbt.nist.gov/garbocki/>) at which the authors first began to formulate their new differential effective medium theory ideas. The work of JGB was performed under the auspices of the U. S. Department of Energy by the Lawrence Livermore National Laboratory under contract No. W-7405-ENG-48 and supported specifically by the Geosciences Research Program of the DOE Office of Energy Research within the Office of Basic Energy Sciences, Division of Engineering and Geosciences.

## References

- [1] D.P. Bentz, E.J. Garboczi, and P.A. Stutzman, in *Interfaces in Cementitious Composites*, edited by J.C. Maso, (E. and F.N. Spon, London, 1993), pp. 259-268. Also found at <http://ciks.cbt.nist.gov/garboczi/>, Chapter 6, Section 3.
- [2] D.P. Bentz, E.J. Garboczi, and E.S. Lagergren, Multi-scale microstructural modelling of concrete diffusivity: Identification of significant variables, *Cement, Concrete, and Aggregates* **20**, 129-139 (1998).
- [3] S. Torquato, *Appl. Mech. Rev.* **44**, 37-76 (1991).
- [4] Z. Hashin, Analysis of composite materials: A survey, *J. Appl. Mech.* **50**, 481-505 (1983).
- [5] J. Dvorkin, J.G. Berryman, and A. Nur, Elastic moduli of cemented sphere packs, *Mech. Mater.* **31**, 461-469 (1999).
- [6] K.L. Scrivener, The Microstructure of Concrete, in *Materials Science of Concrete Vol. I*, edited by J. Skalny (American Ceramic Society, Westerville, OH, 1989), pp. 127-162.
- [7] J.D. Shane, T.O. Mason, H.M. Jennings, E.J. Garboczi, and D.P. Bentz, Effect of the interfacial transition zone on the conductivity of portland cement mortars, *J. Amer. Ceram. Soc.*, in press (1999).
- [8] D.P. Bentz, P.A. Stutzman, and E.J. Garboczi, Experimental and simulation studies of the interfacial zone in concrete, *Cem. Conc. Res.* **22**, 891-902 (1992).
- [9] E.J. Garboczi and D.P. Bentz, Analytical formulas for interfacial transition zone properties, *Advanced Cement-Based Materials* **6**, 99-108 (1997).
- [10] E. Herve and A. Zaoui, *Int. J. Eng. Sci.* **31**, 1-10 (1993).
- [11] M.P. Lutz and P.J.M. Monteiro, in *Microstructure of Cement-Based Systems/Bonding and Interfaces in Cementitious Materials Vol. 370*, edited by S. Diamond, S. Mindess, F.P. Glasser, L.W. Roberts, J.P. Skalny, and L.D. Wakeley (Materials Research Society, Pittsburgh, 1995), pp. 413-418.
- [12] E.J. Garboczi and D.P. Bentz, Multi-scale analytical/numerical theory of the diffusivity of concrete, *Advanced Cement-Based Materials* **8**, 77-88 (1998).
- [13] D.P. Bentz, Influence of silica fume on diffusivity in cement-based materials. II. Multi-scale modelling of concrete diffusivity, submitted to *Cem. Conc. Res.* (1999).

- [14] L.M. Schwartz, E.J. Garboczi, and D.P. Bentz, Interfacial transport in porous media: Application to D.C. electrical conductivity of mortars, *Journal of Applied Physics* **78**, 5898-5908 (1995). Note misprint in eq. 3.1. The corrected form is given here as eq. (8).
- [15] R. McLaughlin, *Int. J. Eng. Sci.* **15**, 237-244 (1977).
- [16] W. Xia and M.F. Thorpe, *Phys. Rev. A* **38**, 2650 (1988).
- [17] D.N. Winslow, M.D. Cohen, D.P. Bentz, K.A. Snyder, and E.J. Garboczi, Percolation and porosity in mortars and concretes, *Cem. Conc. Res.* **24**, 25-37 (1994).
- [18] D.P. Bentz, E.J. Garboczi, and K.A. Snyder, A hard-core soft shell microstructural model for studying percolation and transport in three-dimensional composite media, NIST Internal Report 6265 (1999). Also available at <http://ciks.cbt.nist.gov/garboczi/>, Chapter 6, Section 8.
- [19] E.J. Garboczi, K.A. Snyder, J.F. Douglas, and M.F. Thorpe, Geometrical percolation threshold of overlapping ellipsoids, *Phys. Rev. E* **52**, 819-828 (1995).
- [20] Private communication, D.P. Bentz.
- [21] E.J. Garboczi, D.P. Bentz, and L.M. Schwartz, Modelling the influence of the interfacial zone on the D.C. electrical conductivity of mortar, *Advanced Cement-Based Materials* **2**, 169-181 (1995).
- [22] E.J. Garboczi, Finite element and finite difference programs for computing the linear electric and elastic properties of digital images of random materials, NIST Internal Report 6269 (1998). Also available at <http://ciks.cbt.nist.gov/garboczi/>, Chapter 2.
- [23] <http://ciks.cbt.nist.gov/garboczi/>, Chapter 7, Section 4.
- [24] *Annual Book of ASTM Standards, Concrete and Aggregates*, Vol. 04.02 (American Society for Testing and Materials, West Conshocken, PA, 1995), see *C33* standard.

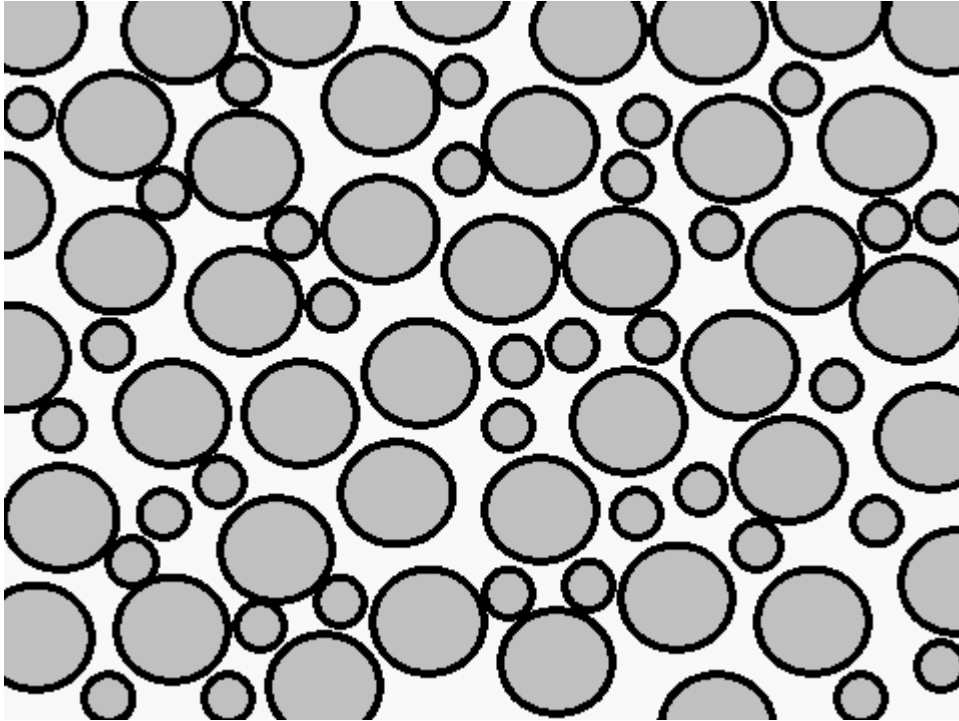


Figure 1: A 2-D schematic view of the concrete composite problem. The dark gray is aggregate, the black is ITZ, and the light gray phase is the bulk matrix phase. There are only two sizes of aggregates in this picture. If the width of the ITZ is  $20\mu\text{m}$ , then the diameters of the particles are about  $100\mu\text{m}$  and  $250\mu\text{m}$ .

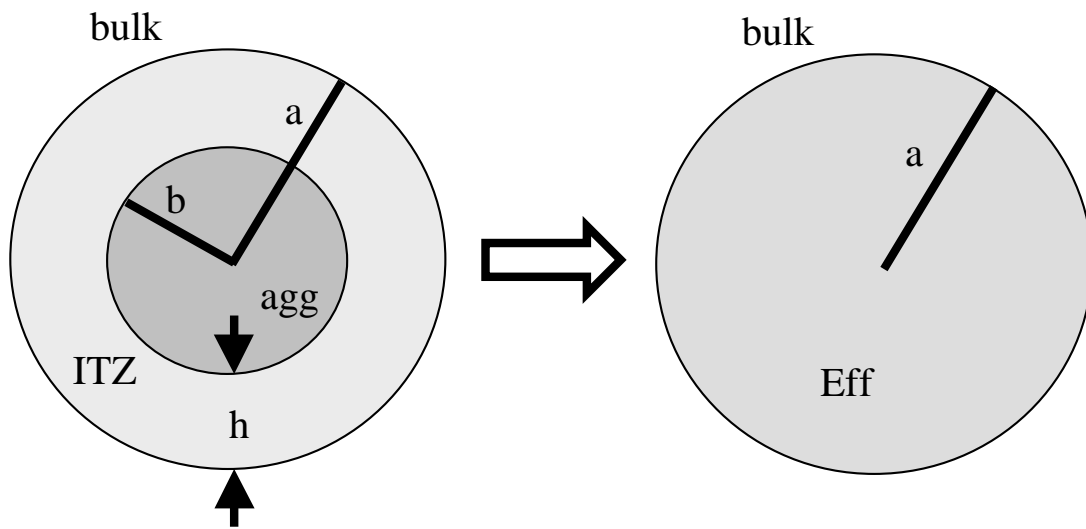


Figure 2: The mapping of a real particle with ITZ into an effective particle whose radius is the radius of the real particle plus the width of the ITZ. The figure also defines the various regions and distances used in the paper.

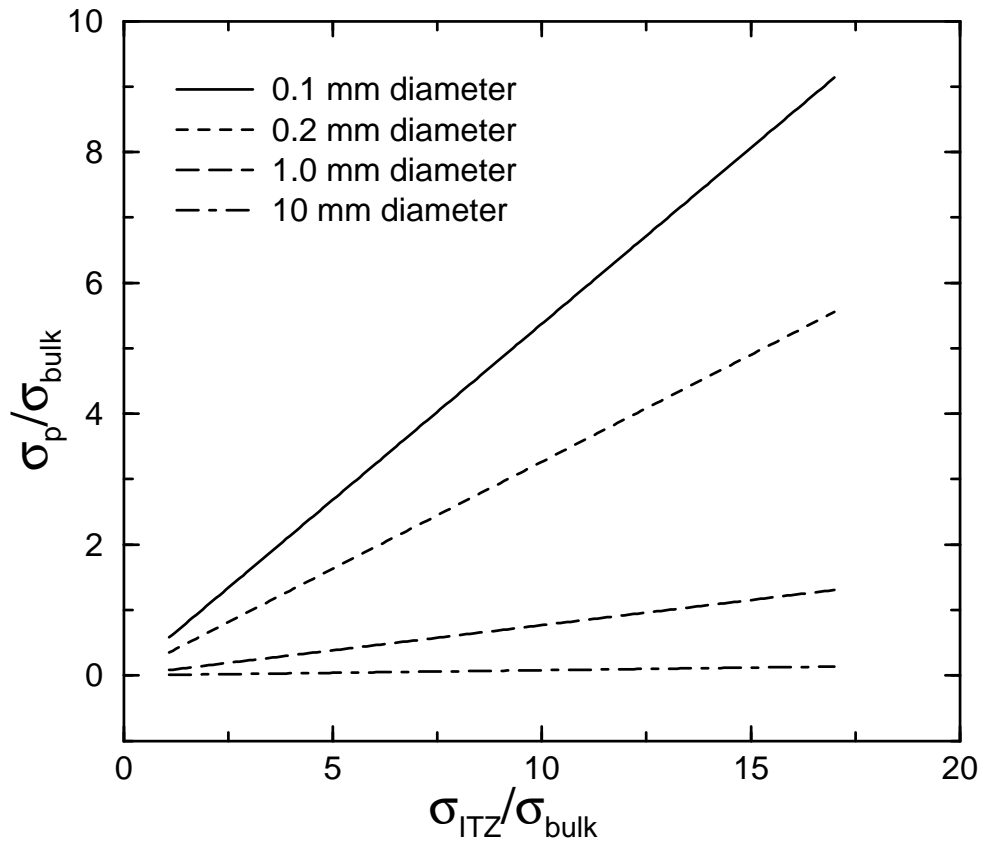


Figure 3: Showing the value of  $\sigma_p/\sigma_{bulk}$ , as a function of the value of  $\sigma_{ITZ}/\sigma_{bulk}$ , for four different diameter aggregate particles (2b), from eq. (13), for  $h = 20\mu\text{m}$ .



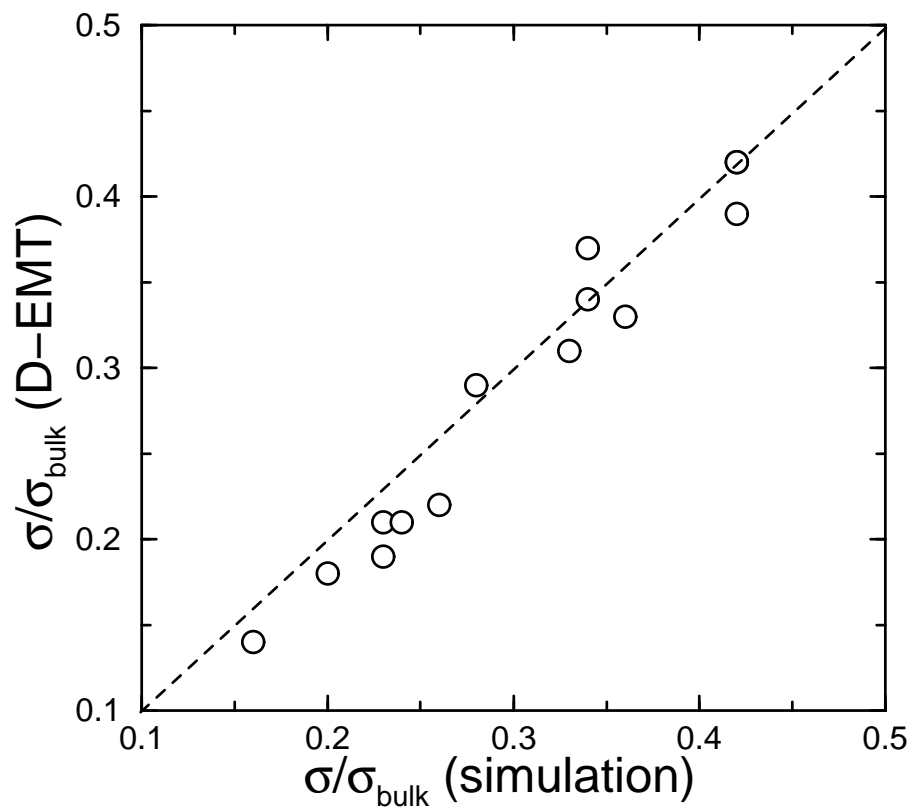


Figure 4: Showing the D-EMT results for  $\sigma/\sigma_{bulk}$  plotted against the simulation results in Table 2. The dashed line is the line of equality.

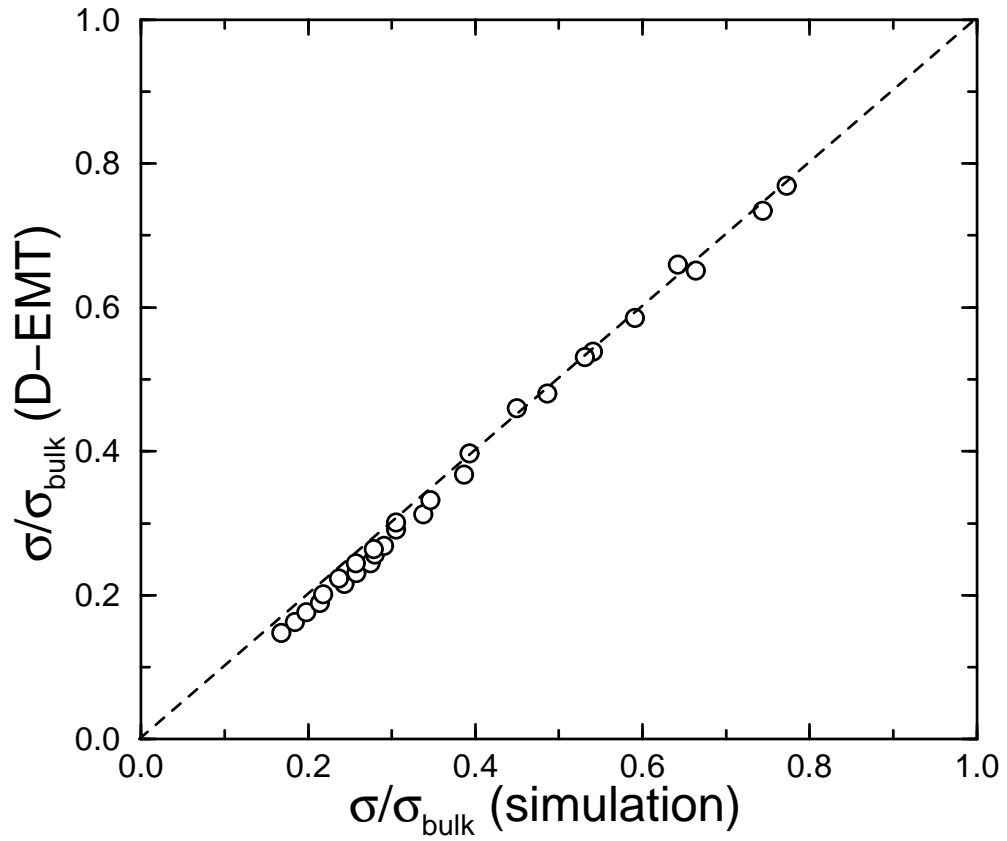


Figure 5: Showing, for the concrete data given in Table 4, the D-EMT results vs. the simulation results for  $\sigma/\sigma_{bulk}$ . The dashed line is the line of equality.

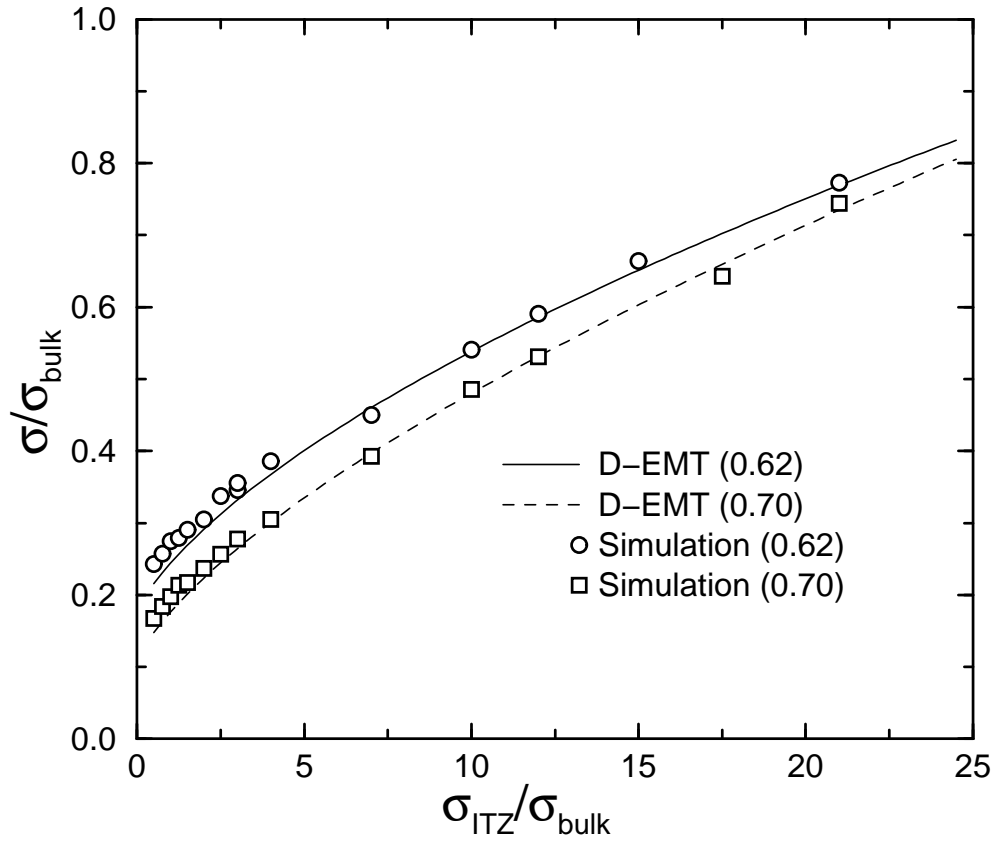


Figure 6: Showing, for the concrete data of Table 4, the overall effective conductivity vs. the the ratio of ITZ to bulk conductivity, for  $V_{agg}$  equal 0.62 and 0.70.

Table 1: Definition of four different sieve analyses used for the concrete systems of Table 2. The numbers given in the table in the four righthand columns are the volume fraction of total aggregate contained in each sieve ( $f_j$ ). Details are given in Ref. [2].

| $d_i$ (mm) | $d_{i+1}$ (mm) | cfcc | ffc  | ffcc | cffc |
|------------|----------------|------|------|------|------|
| 0.075      | 0.15           | 0    | 0.04 | 0.04 | 0    |
| 0.15       | 0.30           | 0.02 | 0.08 | 0.08 | 0.02 |
| 0.30       | 0.60           | 0.08 | 0.12 | 0.12 | 0.08 |
| 0.60       | 1.18           | 0.1  | 0.1  | 0.1  | 0.1  |
| 1.18       | 2.36           | 0.12 | 0.09 | 0.06 | 0.15 |
| 2.36       | 4.75           | 0.06 | 0.06 | 0    | 0.12 |
| 4.75       | 9.525          | 0.26 | 0.33 | 0.24 | 0.35 |
| 9.525      | 12.7           | 0.3  | 0.18 | 0.3  | 0.18 |
| 12.7       | 19.05          | 0.06 | 0    | 0.06 | 0    |

Table 2: Table of parameters for different systems, along with simulation and D-EMT results.

| Sieve Analysis | $c$   | $h(\mu\text{m})$ | $\sigma_{ITZ}/\sigma_{bulk}$ | $\sigma/\sigma_{bulk}$ (simulation) | $\sigma/\sigma_{bulk}$ (D-EMT) | Error(%) |
|----------------|-------|------------------|------------------------------|-------------------------------------|--------------------------------|----------|
| cffc           | 0.753 | 0.01             | 2.95                         | 0.20                                | 0.18                           | -10      |
| cffc           | 0.601 | 0.03             | 4.22                         | 0.42                                | 0.42                           | 0.0      |
| ffc            | 0.754 | 0.03             | 2.54                         | 0.28                                | 0.29                           | 3.6      |
| ffc            | 0.594 | 0.01             | 5.0                          | 0.42                                | 0.42                           | 0.0      |
| ffcc           | 0.602 | 0.01             | 2.84                         | 0.36                                | 0.33                           | -8.3     |
| ffcc           | 0.752 | 0.03             | 3.31                         | 0.34                                | 0.37                           | 8.8      |
| cfcc           | 0.675 | 0.01             | 1.08                         | 0.23                                | 0.19                           | -17.4    |
| cfcc           | 0.675 | 0.01             | 1.88                         | 0.24                                | 0.21                           | -12.5    |
| cfcc           | 0.599 | 0.03             | 2.24                         | 0.34                                | 0.34                           | 0.0      |
| cfcc           | 0.675 | 0.01             | 2.32                         | 0.26                                | 0.22                           | -15.4    |
| cfcc           | 0.524 | 0.01             | 4.06                         | 0.42                                | 0.39                           | -7.1     |
| cfcc           | 0.824 | 0.01             | 4.14                         | 0.16                                | 0.14                           | 12.5     |
| cfcc           | 0.757 | 0.01             | 4.94                         | 0.23                                | 0.21                           | -8.7     |
| cfcc           | 0.675 | 0.01             | 7.53                         | 0.33                                | 0.31                           | -6.1     |

Table 3: Sieve analysis used in the systems of Table 4.

| $d_i$ (mm) | $d_{i+1}$ (mm) | Vol. Frac. of Agg. |
|------------|----------------|--------------------|
| 0.075      | 0.15           | 0.02               |
| 0.15       | 0.30           | 0.05               |
| 0.30       | 0.60           | 0.10               |
| 0.60       | 1.18           | 0.10               |
| 1.18       | 2.36           | 0.105              |
| 2.36       | 4.75           | 0.06               |
| 4.75       | 9.525          | 0.295              |
| 9.525      | 12.7           | 0.240              |
| 12.7       | 19.05          | 0.03               |

Table 4: Table of parameters for different systems, along with simulation and D-EMT results.

| $c$  | $\sigma_{ITZ}/\sigma_{bulk}$ | $\sigma/\sigma_{bulk}$ | D-EMT | % Error |
|------|------------------------------|------------------------|-------|---------|
| 0.70 | 0.5                          | 0.168                  | 0.148 | -11.8   |
| 0.70 | 0.75                         | 0.184                  | 0.163 | -11.4   |
| 0.70 | 1.0                          | 0.198                  | 0.176 | -11.1   |
| 0.70 | 1.25                         | 0.214                  | 0.189 | -11.7   |
| 0.70 | 1.5                          | 0.218                  | 0.201 | -7.8    |
| 0.70 | 2.0                          | 0.237                  | 0.224 | -5.5    |
| 0.70 | 2.5                          | 0.257                  | 0.245 | -4.7    |
| 0.70 | 3.0                          | 0.278                  | 0.264 | -5.0    |
| 0.70 | 4.0                          | 0.305                  | 0.301 | -1.3    |
| 0.70 | 7.0                          | 0.393                  | 0.397 | 1.0     |
| 0.70 | 10.0                         | 0.486                  | 0.480 | -1.2    |
| 0.70 | 12.0                         | 0.531                  | 0.531 | 0.0     |
| 0.70 | 17.5                         | 0.643                  | 0.660 | 2.6     |
| 0.70 | 21.0                         | 0.744                  | 0.735 | -1.2    |
| 0.62 | 0.5                          | 0.243                  | 0.216 | -11.1   |
| 0.62 | 0.75                         | 0.258                  | 0.231 | -10.5   |
| 0.62 | 1.0                          | 0.275                  | 0.244 | -11.3   |
| 0.62 | 1.25                         | 0.279                  | 0.257 | -7.9    |
| 0.62 | 1.5                          | 0.290                  | 0.269 | -7.2    |
| 0.62 | 2.0                          | 0.305                  | 0.292 | -4.3    |
| 0.62 | 2.5                          | 0.337                  | 0.312 | -7.4    |
| 0.62 | 3.0                          | 0.346                  | 0.332 | -4.0    |
| 0.62 | 4.0                          | 0.386                  | 0.368 | -4.7    |
| 0.62 | 7.0                          | 0.450                  | 0.460 | 2.2     |
| 0.62 | 10.0                         | 0.541                  | 0.538 | -0.6    |
| 0.62 | 12.0                         | 0.591                  | 0.586 | -0.8    |
| 0.62 | 15.0                         | 0.664                  | 0.651 | -2.0    |
| 0.62 | 21.0                         | 0.773                  | 0.769 | -0.5    |